Journal of Hazardous Materials 169 (2009) 376–385

Contents lists available at ScienceDirect

Journal of Hazardous Materials

journal homepage: www.elsevier.com/locate/jhazmat

Simultaneous photocatalytic oxidation of As(III) and humic acid in aqueous TiO_2 suspensions

Emmanuil S. Tsimas, Konstantina Tyrovola, Nikolaos P. Xekoukoulotakis, Nikolaos P. Nikolaidis, Evan Diamadopoulos, Dionissios Mantzavinos*

Department of Environmental Engineering, Technical University of Crete, GR-73100 Chania, Greece

ARTICLE INFO

Article history:
Received 28 September 2008
Received in revised form 16 March 2009
Accepted 23 March 2009
Available online 31 March 2009

Keywords:
Arsenic
Factorial design
Humic acid
Photocatalysis
Water

ABSTRACT

The simultaneous photocatalytic oxidation of As(III) and humic acid (HA) in aqueous Degussa P25 TiO_2 suspensions was investigated. Preliminary photocatalytic studies of the binary As(III)/TiO_2 and HA/TiO_2 systems showed that As(III) was oxidized more rapidly than HA and the extent of photocatalytic oxidation of each individual component (i.e. As(III) or HA) increased with decreasing its initial concentration and/or increasing catalyst loading. The simultaneous photocatalytic oxidation of As(III) and HA in the ternary As(III)/HA/TiO_2 system showed that both As(III) and HA oxidation was reduced in the ternary system compared to the corresponding binary systems. The effect of operating conditions in the ternary system, such as initial As(III), HA and TiO_2 concentrations (in the range 3–20 mg/L, 10–100 mg/L and 50–250 mg/L respectively), initial solution pH (3.6–6.7) and reaction time (10–30 min), on photocatalytic As(III) and HA oxidation was assessed implementing a two-level factorial experimental design methodology. Seven and ten factors were found statistically important in the case of photocatalytic As(III) and HA oxidation respectively. Based on these statistically significant factors, a first order polynomial model describing As(III) and HA photocatalytic oxidation was constructed and a very good agreement was obtained between the experimental values and those predicted by the model, while the observed differences may be readily explained as random noise.

1. Introduction

Arsenic is a naturally occurring and ubiquitous element widely distributed in the earth's crust. It can enter groundwater mainly due to natural weathering from arsenic-bearing minerals and sediments in groundwater aquifers [1]. In addition, numerous anthropogenic activities such as mining, coal combustion, and use of pesticides, fertilizers and wood preservatives, also contribute to the arsenic pollution [1]. Arsenic contamination of groundwater is widely recognized as a global public health problem because high levels of arsenic, ranging from tenths to several thousands of μg/L, have been found in groundwater in many regions around the world, including South East Asia, America, and Europe [2]. Consumption of drinking water contaminated with arsenic has been shown to cause urinary bladder, lung and non-melanoma skin cancers, as well as the so-called blackfoot disease [3,4]. Soluble inorganic arsenic occurs in natural waters as trivalent arsenite, As(III), H_3AsO_3, or pentavalent, arsenate, As(V), oxyanions $H_2AsO_4^-$ and $HAsO_4^{2-}$ [5].

Various methods have been developed for the efficient removal of arsenic from drinking water supplies [6–10]. In general, As(V) can be removed more efficiently than As(III) as a result of the stronger adsorption affinity of As(V) oxyanions to solid surfaces compared to the neutral As(III) molecule. Therefore, the oxidation of As(III) to As(V) is required in arsenic removal technologies to increase the removal efficiency of arsenic [11,12]. Among the various chemical oxidants that have been used for the efficient oxidation of As(III) to As(V) [11,12], special emphasis has been given to heterogeneous semiconductor photocatalysis using TiO_2 as a catalyst [12–23]. The mechanism of TiO_2 photocatalysis involves the generation of valence band holes and conduction band electrons upon UV-A illumination of an aqueous TiO_2 suspension and the subsequent generation of hydroxyl $HO^\bullet$ and peroxide $HO_2^\bullet$ radicals [24].

Arsenic contaminated groundwater often contains high levels of humic substances (HS). In arsenic removal technologies using various adsorbent materials, HS may compete with arsenic for the active adsorption sites, thus lowering arsenic removal efficiency. In a recent report, the adsorption of humic acid (HA) onto nanoscale ZVI and its effect on arsenic removal was studied, and it was found that removal efficiency of As(III) and As(V) decreased significantly in the presence of HA [25]. Moreover, in a pilot plant study for the decontamination of arsenic polluted groundwater using gran-

* Corresponding author. Tel.: +30 2821037797; fax: +30 2821037852.
E-mail address: mantzavi@mred.tuc.gr (D. Mantzavinos).

0304-3894/$ – see front matter © 2009 Elsevier B.V. All rights reserved.
doi:10.1016/j.jhazmat.2009.03.107

ular activated alumina/iron(III) hydroxide as an adsorbent in Mako, Hungary, it was found that HA decreased arsenic removal efficiency by blocking active adsorption sites [26].

There are numerous methods available for HA removal, including TiO_2 photocatalytic oxidation [27]. However, there are only few studies in the literature reporting the simultaneous treatment of As(III) and HA. Lee and Choi [15] and Ryu and Choi [16] reported that the addition of HA increased the TiO_2-assisted photocatalytic oxidation of As(III) in acidic but not alkaline pH. The authors suggested that HA enhanced superoxide radicals generation by sensitization, thus enhancing photocatalytic As(III) oxidation. However, the authors did not take into account the photocatalytic oxidation of HA during the course of the reaction. In another recent study, Fostier et al. [28] reported on the photocatalytic arsenic removal using immobilized TiO_2 in PET bottles. The authors studied, among others, the effect of HA on the photocatalytic arsenic removal and they found that As(III) oxidation was reduced in the presence of HA. This finding was explained by the hypothesis that HA competes with arsenic for the photogenerated oxidizing species formed in the reaction. However, the photocatalytic oxidation of HA has been ignored. In another report, Buschmann et al. [29] studied the homogeneous uncatalyzed photo-induced As(III) oxidation in the presence of HA and they found that the presence of HA accelerates the photo-oxidation of As(III). However, again the authors did not take into account the photo-oxidation of HA itself. The same research group also studied the binding of As(III) and As(V) to HA and they found that As(V) was more strongly bound to HA than As(III) [30].

Because As(V) chemical species can be removed more efficiently than As(III), and HA decreases arsenic removal efficiency, a method for the simultaneous As(III) oxidation and HA removal is highly desirable in arsenic removal technologies. The aim of the present work was to perform a detailed study on the simultaneous photocatalytic oxidation of As(III) and HA in aqueous TiO_2 suspensions. The influence of various operating conditions, such as As(III), HA and TiO_2 concentrations, initial solution pH and contact time, on treatment efficiency was evaluated. A two-level factorial design methodology was adopted in order to determine the statistical significance of each parameter, their possible interactions, and to provide a simple mathematical model describing the simultaneous photocatalytic oxidation of As(III) and HA in aqueous TiO_2 suspensions. To the best of our knowledge, such a detailed study on the factors affecting the simultaneous photocatalytic oxidation of As(III) and HA in aqueous TiO_2 suspensions has not been performed.

2. Experimental

2.1. Solution preparation

Solutions were prepared in ultra pure water (resistivity 18.2 MΩ cm at 25 °C) prepared on a water purification system (EASYpureRF) supplied by Barnstead/Thermolyne (USA). As(III) and As(V) stock solutions (1000 mg/L) were prepared by dissolving the appropriate amounts of $NaAsO_2$ (Fluka) and $Na_2HAsO_4{\cdot}7H_2O$ (Fluka) respectively in ultra pure water acidified with HCl (2–5% final concentration) and were stored in the refrigerator at 4 °C. HA sodium salt was purchased from Aldrich and used as received without further purification. Although the limitations of using Aldrich HA or, indeed, similar commercially available products, as an accurate representative of natural terrestrial humic substances have been highlighted by Malcolm and MacCarthy [31], their use is very common in studies dealing with various environmental aspects of HA [32–35].

HA stock solutions (1000 mg/L) were prepared by dissolving the appropriate amount of HA in 1 M NaOH solution because HA dissolution is favored at alkaline conditions [36], and then diluted with ultra pure water and stored in the refrigerator at 4 °C. Prior to the photocatalytic experiments, arsenic and HA stock solutions were diluted and mixed to achieve the desired final concentrations of arsenic and HA and solution pH was adjusted by the addition of appropriate amounts of 1 M NaOH or $HClO_4$ solution as needed. It should be noted that although humic acid is insoluble in dilute acidic solutions [36], at the experimental conditions used in the present study (i.e. at pH = 3 and humic acid concentration in the range 10–100 mg/L), no precipitation of humic acid in the reaction solution was observed.

2.2. Photocatalytic experiments

The TiO_2 photocatalyst employed in the present study was Degussa P25 kindly supplied by Degussa AG (anatase:rutile 75:25, 21 nm primary crystallite particle size, 0.4–3 μm aggregate particle size [37], 50 m^2/g BET area). UV-A irradiation was provided by a 9 W lamp (Radium Ralutec, 9W/78) emitting predominantly at 350–400 nm. The photon flux emitted from the lamp was determined actinometrically using the potassium ferrioxalate method and was found 4.69×10^{-6} einstein/s. Experiments were conducted in an immersion well, batch type, laboratory scale photoreactor, purchased from Ace Glass (Vineland, NJ, USA) and described in detail elsewhere [38]. In a typical photocatalytic run, 350 mL of the aqueous sample containing the desired concentrations of As(III) and HA were loaded in the reaction vessel. The solution was slurried with the appropriate amount of catalyst and magnetically stirred for 30 min in the dark to ensure complete equilibration of adsorption/desorption of arsenic and HA onto the TiO_2 surface. After that period, the UV-A lamp was turned on, while pure O_2 was continuously sparged in the liquid and the reaction mixture was continuously stirred. The pH of the solution was practically constant during the course of the reaction. Samples periodically taken from the reactor were filtered (with 0.45 μm disposable filters) to remove catalyst particles and then analyzed for their residual arsenic and HA concentration which was subtracted from the total concentration to compute the extent of arsenic and HA conversion.

2.3. Analytical measurements

The whole absorbance spectrum (i.e. from 200 to 700 nm) of the reaction mixtures was recorded on a UV/Vis Shimadzu UV 1240 spectrophotometer. HA concentration was measured monitoring sample absorbance at three different wavelengths, namely 254, 350 and 436 nm using respective calibration curves; these were constructed measuring the absorbance of several HA solutions of known concentration. It was found that the discrepancy in HA concentration measured at these three wavelengths was always less than 5%. According to these findings, HA concentration was computed based on the calibration curve at 254 nm. It should be noted that special emphasis is given on the absorbance at 254 nm because it has been found that the absorbance at this wavelength is a good surrogate parameter for monitoring total organic carbon concentration of organic matter in natural waters [39]. As the absorbance of HA solutions is pH-dependent, the same procedure was followed at acidic conditions (i.e. pH = 3) and a separate calibration curve was used.

On the other hand, arsenic speciation analysis was performed using an anion exchange method adopted by Meng et al. [40] using disposable cartridges packed with 2.5 g of selective aluminosilicate adsorbent, supplied by Metalsoft Center, NJ, USA. Arsenic speciation was performed by passing 10 mL of sample through the cartridges. The cartridges retain As(V) while As(III) passes through the adsorbent. As(III) concentration was measured by analyzing the sample passing through the ion exchange resin using a modified colorimetric molybdate-blue method developed by Dhar et al. [41] with

a detection limit of 35 μg/L. This method is based on the fact that As(V) forms a complex with reduced molybdate that strongly absorbs in the infrared, while As(III) does not.

The method requires the preparation of an oxidizing solution containing 2 mmol/L KIO_3 in 2% hydrochloric acid. The color reagent that is added to the oxidized sample aliquot requires the preparation of the following aqueous solutions: 10.8% L-ascorbic acid $C_6H_8O_6$ (613 mmol/L), 3% ammonium molybdate $(NH_4)_6Mo_7O_{24}{\cdot}4H_2O$ (24 mmol/L), 0.56% antimony potassium tartrate $C_8H_4K_2O_{12}Sb_2{\cdot}3H_2O$ (8 mmol/L), and 13.98% H_2SO_4 (2.5 mmol/L). To form the color reagent, the solutions of ascorbic acid, ammonium molybdate, and potassium antimonyl tartrate were first combined, while the sulfuric acid solution must be added to the mixed solution immediately after the addition of potassium antimonyl tartrate to avoid the generation of turbidity in the color reagent. The mixing ratios of the four reagents forming the color solution were 2:2:1:5 respectively.

The experimental procedure for the determination of As(III) concentration was as follows: 0.5 mL of the oxidizing solution was added to 5 mL of the sample after passing through the adsorbent cartridge, to oxidize As(III) to As(V). After 20 min, 0.5 mL of the color reagent was added to the above solution and the resulting solution was thoroughly mixed by shaking and it was left in the dark for 60 min to complete the color forming complexation reaction. Sample absorbance was measured at 880 nm on a UV/Vis Shimadzu UV 1240 spectrophotometer. According to the above procedure, a calibration curve was constructed by measuring the absorbance of As(V) complex derived from As(III) solutions of known concentration.

2.4. Experimental design

In the present work, a statistical approach was chosen based on a two-level factorial experimental design [42] that would allow us to infer about the effect of the variables and their interactions with a relatively small number of experiments. In a two-level factorial design, each variable assumes two values or levels, a high one and a low one. Five independent variables were considered, namely: As(III), HA and TiO_2 concentration in mg/L, initial pH of the solution and treatment time. Regarding the initial concentrations of As(III) employed in the factorial design, these were 3 and 20 mg/L. It should be noted that arsenic concentrations of 10 mg/L or higher have been reported in environmental samples although they do not usually exceed 1 mg/L [1,2]. The reason why As(III) concentrations considerably greater than those typically found in waters (although of the same order of magnitude) were chosen was to allow (i) the assessment of process efficiency within a measurable time scale and (ii) the accurate determination of residual concentrations with the analytical techniques employed in this work. For HA, initial concentrations were 10 and 100 mg/L; these values are in accordance with HA environmental concentrations that may reach values as high as 200 mg/L of dissolved organic carbon [43].

The two measured response factors (dependent variables) were concentration of As(III) oxidized (response factor Y_1) and concentration of HA oxidized (response factor Y_2). All possible combinations of the five variables at two levels give rise to $2^5 = 32$ experimental runs. The order each experiment was performed was selected randomly. The various statistical parameters were computed using the statistical package Minitab 14.

3. Results and discussion

3.1. Adsorption studies

Preliminary blank experiments were conducted to assess the extent of As(III) and HA adsorption onto the TiO_2 surface in the dark and the results are summarized in Table 1. Adsorption experiments were monitored for 60 min and in all cases it was found that the equilibrium between adsorption/desorption was established in about 20 min. For the binary As(III)/TiO_2 system, adsorption at 3 mg/L initial As(III) concentration increased from 7 to 21 to 35% as a result of increasing catalyst loading from 100 to 250 to 500 mg/L at pH = 6.5, while the effect of lowering pH was marginal. For the binary HA/TiO_2 system, its adsorption onto TiO_2 surface was favored at acidic pH = 3.9, at high TiO_2 loadings and low HA initial concentration. The highest HA adsorption, at the present experimental conditions, was 43% and it was observed at 10 mg/L initial HA concentration, 250 mg/L TiO_2 loading and acidic pH. For the ternary As(III)/HA/TiO_2 system, As(III) adsorption remained practically unaffected by the presence of HA; interestingly though, HA adsorption was enhanced possibly due to interactions between As(III), HA and the catalyst surface.

3.2. Photocatalytic oxidation of the binary As(III)/TiO_2 system

In further experiments, the photocatalytic oxidation of As(III) in the binary As(III)/TiO_2 system was studied at 50 mg/L TiO_2 loading, pH = 6.4 and initial As(III) concentrations in the range 3–20 mg/L

Table 1
Percent adsorption of As(III) and HA onto the surface of TiO_2 at various experimental conditions in the dark.

Experimental conditions				As(III) adsorption, %	HA adsorption, %
[As(III)], mg/L	[HA], mg/L	[TiO_2], mg/L	pH		
3	–	100	6.5	7	–
3	–	500	6.5	35	–
3	–	50	6.5	5	–
3	–	250	6.5	21	–
3	–	50	3.9	6	–
3	–	250	3.9	15	–
–	10	50	6.5	–	12
–	10	250	6.5	–	17
–	10	50	3.9	–	19
–	10	250	3.9	–	43
3	10	50	6.5	4	36
3	10	250	6.5	16	52
3	10	50	3.9	4	62
3	10	250	3.9	12	93
–	100	50	6.5	–	3
–	100	50	3.9	–	7
–	100	250	6.5	–	5
–	100	250	3.9	–	23

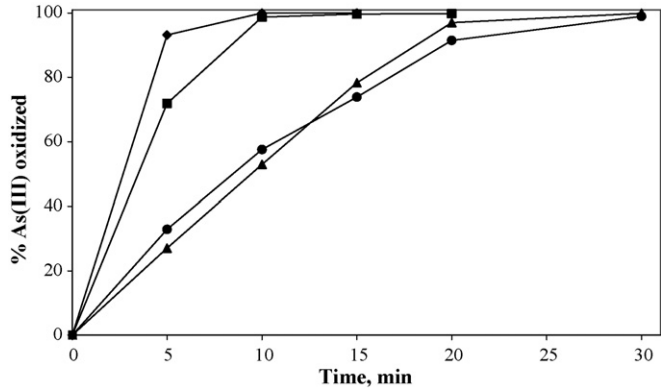

Fig. 1. Photocatalytic oxidation of As(III) at 50 mg/L TiO_2 loading, pH = 6.4 and various initial As(III) concentrations: (♦) $[As(III)]_0$ = 3 mg/L; (■) $[As(III)]_0$ = 5 mg/L; (▲) $[As(III)]_0$ = 10 mg/L; and (●) $[As(III)]_0$ = 20 mg/L.

and the results are shown in Fig. 1. Preliminary blank experiments were performed by sparging pure oxygen in the reaction vessel in the absence of TiO_2 and it was found that the concentration of As(III) was practically constant at the time scale used in the present experiments, i.e. 30 min treatment time (data not shown). As(III) photocatalytic oxidation proceeds relatively fast even for the higher As(III) concentration tested. When the initial As(III) concentration was 3 mg/L, complete As(III) oxidation (i.e. As(III) concentration was below the detection limit) was accomplished in 10 min, while at initial As(III) concentrations of 5 and 10 mg/L complete (i.e. As(III) concentration was below the detection limit) photocatalytic oxidation was achieved in 15 and 30 min respectively. Further increase of initial As(III) concentration from 10 to 20 mg/L resulted in practically the same concentration–time profile for As(III) oxidation. From the above results it can be concluded that for initial As(III) concentrations in the range 3–20 mg/L, photocatalytic oxidation can be accomplished within 10–30 min.

3.3. Photocatalytic oxidation of the binary HA/TiO_2 system

In additional experiments, the photocatalytic oxidation of HA in the binary system HA/TiO_2 was studied at 10 and 50 mg/L initial HA concentrations, TiO_2 loadings in the range 50–500 mg/L and pH = 6.3 and the results are shown in Fig. 2. As can be seen, photocatalytic HA oxidation is a relatively slow process compared to As(III) oxidation. For instance, at 10 mg/L initial HA concentration and 50 mg/L TiO_2 loading, complete HA oxidation was achieved after 60 min of treatment. Moreover, increasing catalyst loading at

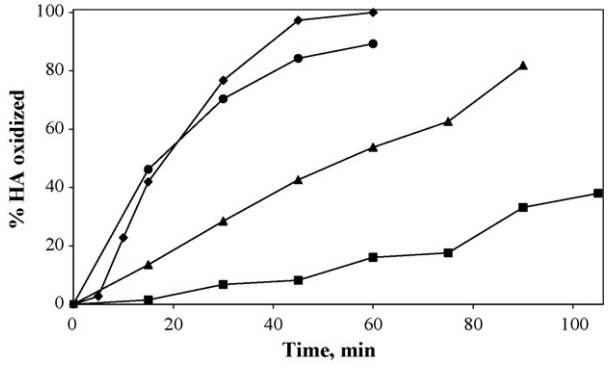

Fig. 2. Photocatalytic oxidation of HA at pH = 6.3 and various initial HA concentrations and TiO_2 loadings: (♦) $[HA]_0$ = 10 mg/L, $[TiO_2]$ = 50 mg/L; (■) $[HA]_0$ = 50 mg/L, $[TiO_2]$ = 50 mg/L; (▲) $[HA]_0$ = 50 mg/L, $[TiO_2]$ = 100 mg/L; and (●) $[HA]_0$ = 50 mg/L, $[TiO_2]$ = 500 mg/L.

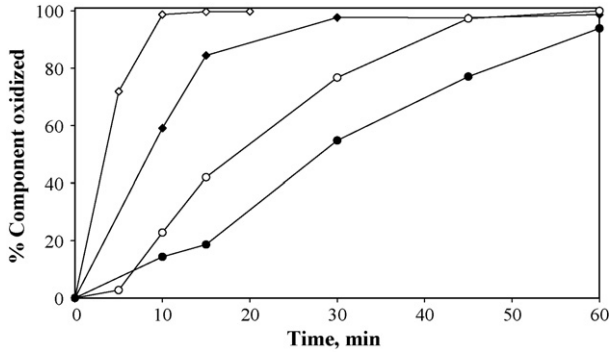

Fig. 3. Photocatalytic oxidation of As(III) and HA at 50 mg/L TiO_2 loading and pH = 6.4: (◊) As(III) oxidation in the binary As(III)/TiO_2 system for $[As(III)]_0$ = 5 mg/L; (♦) As(III) oxidation in the ternary As(III)/HA/TiO_2 system for $[As(III)]_0$ = 5 mg/L and $[HA]_0$ = 10 mg/L; (○) HA oxidation in the binary HA/TiO_2 system for $[HA]_0$ = 10 mg/L; and (●) HA oxidation in the ternary As(III)/HA/TiO_2 system for $[As(III)]_0$ = 5 mg/L and $[HA]_0$ = 10 mg/L.

a common initial HA concentration resulted in increased HA photocatalytic oxidation; for example, increasing catalyst loading from 50 to 100 and then to 500 mg/L at 50 mg/L initial HA concentration, resulted in 7, 28.5 and 70.5% HA oxidation respectively after 30 min treatment time. On the other hand, increasing HA concentration from 10 to 50 mg/L at a common catalyst loading of 50 mg/L resulted in decreased HA photocatalytic oxidation. From the above preliminary studies, it can be concluded that As(III) is oxidized more rapidly than HA, with the extent of photocatalytic oxidation of each individual component (i.e. As(III) or HA) increasing with decreasing its initial concentration and/or increasing catalyst loading.

3.4. Photocatalytic oxidation of the ternary As(III)/HA/TiO_2 system

In further studies, the simultaneous photocatalytic oxidation of As(III) and HA in the ternary As(III)/HA/TiO_2 system was monitored for 60 min at 50 mg/L TiO_2 loading, pH = 6.4, and initial As(III) and HA concentrations of 5 and 10 mg/L respectively and the results are shown in Fig. 3. For comparison, Fig. 3 also shows the corresponding results for the binary As(III)/TiO_2 and HA/TiO_2 systems at common initial As(III) and HA concentrations, TiO_2 loading and solution pH. As can be seen, As(III) photocatalytic oxidation decreased in the presence of HA. For instance, after 10 min treatment time, As(III) photocatalytic oxidation in the binary As(III)/TiO_2 system was about 98% and it was reduced to about 60% in the presence of 10 mg/L HA in the ternary As(III)/HA/TiO_2 system. Moreover, HA photocatalytic oxidation was also reduced in the presence of As(III), but to a lower extent compared to the reduction of the As(III) photocatalytic oxidation in the presence of HA. For example, after 30 min treatment time, HA photocatalytic oxidation in the binary HA/TiO_2 system was about 77% and it was reduced to about 55% in the presence of 5 mg/L As(III) in the ternary As(III)/HA/TiO_2 system. The reason for the observed decreased photocatalytic oxidation of As(III) and HA in the ternary system may be the competition between As(III) and HA for the available photogenerated oxidizing species (i.e. valence band holes, hydroxyl radicals and other reactive oxygen species), which at a fixed set of photocatalytic conditions, are generated at a constant rate. Such competition will result in decreased photocatalytic oxidation efficiency compared with the binary systems. Regarding HA transformation, one could speculate that it predominantly occurs through radical reactions in the liquid bulk rather than onto the catalyst surface since a substantial enhancement of its adsorption in the ternary system (Table 1) is accompanied by lower conversions. It should be noted that such a decreased photocatalytic activity of the ternary system was also observed in a recent

study concerning the photocatalytic transformation of the azo dye acid orange 20 and Cr(VI) oxyanions [44].

In recent studies, Lee and Choi [15] and Ryu and Choi [16] suggested a pathway for the TiO_2-mediated photocatalytic oxidation of As(III) involving the participation of superoxide radical as the primary but not exclusive oxidant (this was evidenced through experiments with superoxide and hydroxyl radical scavengers). They also reported that the presence of HA increased As(III) oxidation at acidic conditions (pH = 3) but had no effect at alkaline conditions (pH = 9). It was hypothesized that HA was first photosensitized and then reacted with oxygen to enhance the formation of superoxide radical. This eventually enhanced As(III) oxidation at acidic conditions, where the rate of superoxide radical formation and consequently its oxidizing ability are relatively low compared to those at alkaline conditions. They also reported [15] that As(III) oxidation would be reduced in the presence of HA if hydroxyl radicals and valence band holes rather than superoxide radicals were the dominant oxidizing species and this is what we observed in the present study. This has also been observed by Dutta et al. [17] who studied the effect of benzoic and formic acids as competitive substrates on As(III) photocatalytic oxidation; they found that the rate of the TiO_2 photocatalytic transformation of As(III) and the organic acid in the ternary system was lower than that in the respective binary systems, thus confirming the dominant role of hydroxyl radicals and valence band holes in the process. The fact that the photosensitizing contribution of HA seems not to be critical in our work may be associated with the experimental conditions involved and, in particular, the irradiation source. In this work, a 9 W fluorescent lamp emitting in the UV-A region only was employed, while Lee and Choi [15] and Ryu and Choi [16] employed a 300 W xenon arc lamp emitting in the UV-A/Vis region (>300 nm); this could possibly affect the photocatalytic mechanisms and pathways involved. Other differences include the level of As(III) and TiO_2 concentrations, the reactor geometry and liquid holdup and the water matrix all of which can affect photocatalytic performance.

It should be pointed out that the issue of As(III) photocatalytic oxidation is highly controversial and there is no consensus about what plays the role of the main oxidant. In fact, the As(III) TiO_2-induced photocatalytic oxidation provides a unique example in which the mechanism sensitively depends on the reaction conditions, the presence of competitive substrates and the catalyst properties [22]. In the presence of HA, for instance, the chemistry of the photocatalytic transformations may involve complex reaction pathways and mechanisms based on e.g. interactions of As(III) with organic radicals arising from HA degradation, interactions of HA with metal complexes associated with As(III) oxidation and, even, reductive HA conversion through its reaction with conduction band electrons. In this respect, a detailed mechanistic approach was outside the scope of this work.

3.5. Factorial experimental design

To investigate further the various parameters affecting the simultaneous photocatalytic oxidation of As(III) and HA in the ternary As(III)/HA/TiO_2 system as well as their possible interactions, a statistical approach based on factorial experimental design at two levels was chosen [42]. In the present study, five independent variables that may affect the simultaneous photocatalytic oxidation of As(III) and HA were taken into account, namely As(III), HA and TiO_2 concentrations, initial pH of the solution and treatment time. The values chosen for the independent variables and the results obtained in terms of two measured response factors (dependent variables), namely concentration of As(III) oxidized (response factor Y_1) and concentration of HA oxidized (response factor Y_2) are presented in Table 2. It should be noted that the concentration of oxidized As(III) and HA rather than the respective percent removal was chosen as response factors, because concentration is more representative than removal for runs conducted at different initial concentrations. The low and high values for each variable were chosen according to the preliminary results.

Table 2
Design matrix of the 2^5 factorial experimental design and results obtained in terms of As(III) oxidized (response factor Y_1) and HA oxidized (response factor Y_2).

Standard order	X_1 [As(III)], mg/L	X_2 [HA], mg/L	X_3 [TiO_2], mg/L	X_4 pH	X_5 reaction time, min	Y_1 As(III) oxidized, mg/L	Y_2 HA oxidized, mg/L
1	3	10	50	3.6	10	0.91	4.95
2	20	10	50	3.6	10	1.29	5.77
3	3	100	50	3.6	10	0.32	18.09
4	20	100	50	3.6	10	1.42	11.65
5	3	10	250	3.6	10	2.86	9.11
6	20	10	250	3.6	10	12.21	7.38
7	3	100	250	3.6	10	1.07	28.34
8	20	100	250	3.6	10	0.00	31.86
9	3	10	50	6.7	10	2.62	0.76
10	20	10	50	6.7	10	5.75	1.26
11	3	100	50	6.7	10	0.77	5.81
12	20	100	50	6.7	10	0.25	3.15
13	3	10	250	6.7	10	2.95	7.89
14	20	10	250	6.7	10	16.21	7.35
15	3	100	250	6.7	10	2.85	5.45
16	20	100	250	6.7	10	8.73	12.90
17	3	10	50	3.6	30	2.61	8.07
18	20	10	50	3.6	30	7.17	5.87
19	3	100	50	3.6	30	0.48	14.91
20	20	100	50	3.6	30	2.79	11.87
21	3	10	250	3.6	30	2.97	9.89
22	20	10	250	3.6	30	19.41	9.24
23	3	100	250	3.6	30	2.27	29.75
24	20	100	250	3.6	30	5.39	35.10
25	3	10	50	6.7	30	3.00	3.06
26	20	10	50	6.7	30	11.83	3.51
27	3	100	50	6.7	30	1.69	5.39
28	20	100	50	6.7	30	2.42	4.46
29	3	10	250	6.7	30	2.97	9.84
30	20	10	250	6.7	30	19.27	10.37
31	3	100	250	6.7	30	2.98	13.36
32	20	100	250	6.7	30	18.50	16.24

Table 3
Average and main effects of the independent variables and their two and higher order interactions of the 2^5 factorial design on the response factors Y_1 and Y_2.

Effect	Value of effect	
	Oxidation of As(III)	Oxidation of HA
Average effect	5.187 ± 0.445	11.009 ± 0.557
Main effects		
[As(III)]	6.206 ± 0.89	0.229 ± 1.115
[HA]	−3.885 ± 0.89	9.024 ± 1.115
[TiO_2]	4.707 ± 0.89	8.491 ± 1.115
pH	2.477 ± 0.89	−8.168 ± 1.115
Reaction time	2.847 ± 0.89	1.848 ± 1.115
Two-factor interactions		
[As(III)] × [HA]	−2.822 ± 0.89	0.537 ± 1.115
[As(III)] × [TiO_2]	3.643 ± 0.89	1.871 ± 1.115
[As(III)] × pH	1.682 ± 0.89	0.731 ± 1.115
[As(III)] × Time	2.269 ± 0.89	0.07 ± 1.115
[HA] × [TiO_2]	−0.751 ± 0.89	3.718 ±1.115
[HA] × pH	0.58 ± 0.89	−6.183 ± 1.115
[HA] × Time	−0.208 ± 0.89	−0.12 ± 1.115
[TiO_2] × pH	1.057 ± 0.89	−1.491 ± 1.115
[TiO_2] × Time	0.511 ± 0.89	1.09 ± 1.115
pH × Time	−0.028 ± 0.89	0.859 ± 1.115
Three-factor interactions		
[As(III)] × [HA] × [TiO_2]	−1.165 ± 0.89	2.161 ± 1.115
[As(III)] × [HA] × pH	0.337 ± 0.89	0.188 ± 1.115
[As(III)] × [HA] × Time	−0.23 ± 0.89	0.23 ± 1.115
[As(III)] × [TiO_2] × pH	1.206 ± 0.89	−0.252 ± 1.115
[As(III)] × [TiO_2] × Time	0.726 ± 0.89	−0.143 ± 1.115
[As(III)] × pH × Time	0.185 ± 0.89	−0.297 ± 1.115
[HA] × [TiO_2] × pH	1.969 ± 0.89	−3.433 ± 1.115
[HA] × [TiO_2] × Time	0.97 ± 0.89	1.155 ± 1.115
[HA] × pH × Time	0.638 ± 0.89	0.447 ± 1.115
[TiO_2] × pH × Time	−0.087 ± 0.89	0.257 ± 1.115
Four-factor interactions		
[As(III)] × [HA] × [TiO_2] × pH	1.611 ± 0.89	−0.302 ± 1.115
[As(III)] × [HA] × [TiO_2] × Time	0.694 ± 0.89	−0.84 ± 1.115
[As(III)] × [HA] × pH × Time	0.501 ± 0.89	−0.712 ± 1.115
[As(III)] × [TiO_2]× pH × Time	−0.01 ± 0.89	−0.504 ± 1.115
[HA] × [TiO_2]× pH × Time	0.305 ± 0.89	0.087 ± 1.115
Five-factor interactions		
[As(III)] × [HA] × [TiO_2] × pH × Time	0.688 ± 0.89	−0.087 ± 1.115
Lenth's PSE	1.032	0.67
ME	2.288	1.486

Statistical treatment of the response factors Y_1 and Y_2 according to the factorial design technique involves the estimation of the average effect, the main effects of each individual variable as well as their two and higher order interaction effect. The average effect is the mean value of each response factor, while the main and interaction effects are the difference between two averages: main effect = $\overline{Y_+} - \overline{Y_-}$, where $\overline{Y_+}$ and $\overline{Y_-}$ are the average response factors at the high and low level respectively of the independent variables or their interactions. Estimation of the average effect, as well as the main and interaction effects was made by means of the statistical package Minitab 14 and the results are summarized in Table 3.

A key element in the factorial design statistical procedure is the determination of the significance of the estimated effects. To assess the significance of the effects, an estimate of the standard error is required. An estimate of the standard error is usually made by performing repeat runs. Alternatively, three and higher order interactions can be used because these interactions may be considered negligible and may measure differences arising from experimental error [42]. The variance of each effect would then be

$$\text{Variance\_of\_effects} = \frac{\sum(\text{three\_and\_higher\_order\_effect})^2}{\text{number\_of\_three\_and\_higher\_order\_effects}} \quad (1)$$

The standard error is then the square root of the variance (half this amount for the average). The estimated standard error for each variable and interaction appears in Table 3. If an effect is about or below the standard error, it may be considered insignificant (or in

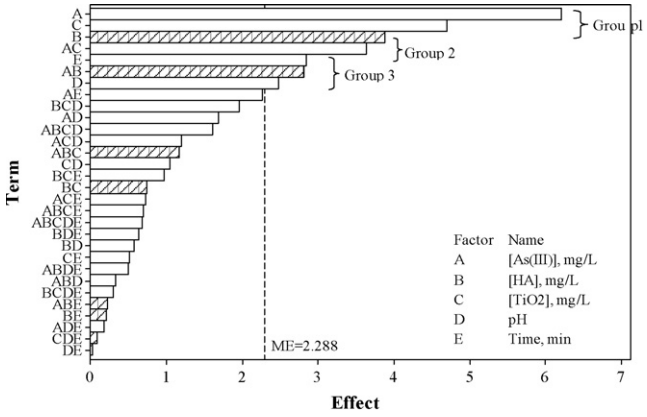

Fig. 4. Pareto chart of the effects for As(III) oxidation. White bars: positive effects; hatched bars: negative effects. The dotted line is drawn at the margin of error (ME).

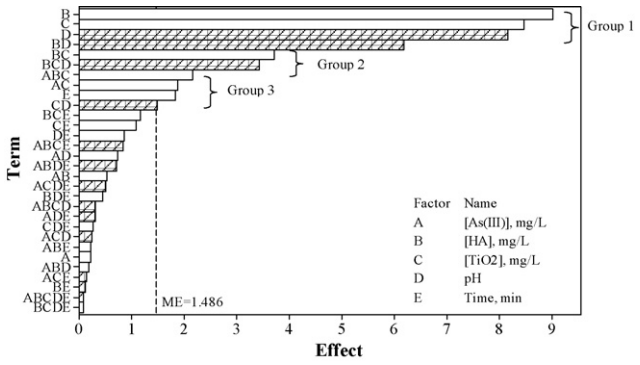

Fig. 5. Pareto chart of the effects for HA oxidation. White bars: positive effects; hatched bars: negative effects. The dotted line is drawn at the margin of error (ME).

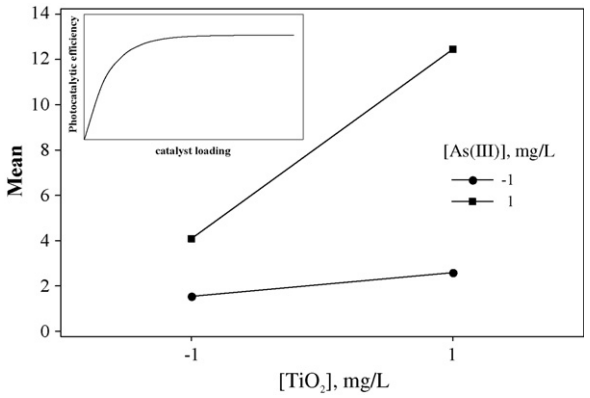

Fig. 6. Interaction plot for [As(III)] × [TiO_2]. Abscissa: TiO_2 concentration in coded units. Ordinate: mean of response factor Y_1 at the designated values of the variables [As(III)] and [TiO_2]; (●) effect of increasing [TiO_2] at the low level of [As(III)]; (■) effect of increasing [TiO_2] at the high level of [As(III)]. Inset: effect of catalyst loading on the photocatalytic efficiency.

other terms, not different from zero). The contribution of a variable, however, whose effect appears different from zero, is not necessarily very large. One way to identify the significance of the main and interaction effects in un-replicated factorial designs is to apply the Lenth's pseudo standard error (PSE) [42,45]. Lenth's PSE is an estimate of the standard error of the effects and for its calculation the median, m, of the absolute values of the effects is first determined and then PSE = 1.5*m*. Any estimated effect exceeding 2.5 × PSE is excluded and, if needed, *m* and PSE are recalculated. Then, a margin of error (ME) is given by ME = t × PSE, where t is the (1 − alpha/2) quantile of a t-distribution with degrees of freedom equal to the number of effects/3 [42,45]. The present study was done for a confidence interval of 95%, therefore alpha = 0.05. The calculated values of PSE and ME for the two response factors according to the Minitab software are also given in Table 3. All estimated effects greater than the ME can be considered significant. On the other hand, all the other effects whose values are lower than the ME can be attributed to random statistical error.

3.6. Pareto chart of the effects

A very useful pictorial presentation of the estimated effects and their statistical importance can be accomplished using the Pareto chart of the effects. The Pareto chart displays the absolute values of the effects in the ordinate, while a reference line is drawn at the margin of error, and any effect exceeding this reference line is potentially important. The Pareto charts of the effects for the As(III) and HA oxidation are shown in Figs. 4 and 5 respectively. As can be seen in Fig. 4, there are basically seven effects which are statistically important for As(III) oxidation, namely, in decreasing order of significance: [As(III)], [TiO_2], [HA], the interaction effect of [As(III)] × [TiO_2], treatment time, the interaction effect of [As(III)] × [HA] and the pH of the solution. These effects are the most important factors affecting the oxidation of As(III) in the ternary As(III)/HA/TiO_2 system. All the other effects are not significant and may be explained as random noise.

A closer look at Fig. 4 indicates that there are three groups of significant effects. The first group comprises the two largest positive effects of As(III) and TiO_2 concentration. The large positive effect of these factors indicates that increasing their values increases As(III) oxidation. These results can be easily explained because increasing the concentration of As(III) relative to the concentration of HA increases the amount of As(III) available for oxidation. Moreover, increasing TiO_2 concentration increases the active sites onto the catalyst surface as well as the photogenerated oxidizing species available for photocatalytic oxidation of As(III).

The second group of significant effects comprises a medium negative effect of HA concentration and a medium positive interaction effect of [As(III)] × [TiO_2]. The negative effect of HA concentration indicates that increasing HA concentration prevents As(III) oxidation. This effect may be attributed to the competition between As(III) and HA for adsorption onto the catalyst surface and their subsequent photocatalytic oxidation. The positive interaction effect of [As(III)] × [TiO_2] implies a synergistic effect between As(III) and TiO_2 concentrations and can be interpreted in terms of the interaction plot shown in Fig. 6. The slopes of the lines in the interaction plot of [As(III)] × [TiO_2] show the effect of increasing TiO_2 loading at the high and low levels of As(III) concentration, and the difference between the two slopes gives the interaction effect of [As(III)] × [TiO_2]. If the lines are parallel or close to parallel then the interaction effect will be zero or close to zero. On the other hand, if the lines have different slopes this indicates an interaction effect between the two variables. As can be seen in Fig. 6, the effect of increasing TiO_2 loading at the low level of As(III) concentration is lower than that at the high level of As(III) concentration. This means that increasing TiO_2 loading at the high level of As(III) concentration has a higher impact on the amount of As(III) oxidized.

A possible explanation can be given in terms of the effect of catalyst loading on the photocatalytic efficiency. In general, photocatalytic efficiency increases by increasing catalyst loading up to a certain value, above which photocatalytic efficiency levels off and becomes practically independent of catalyst loading, as can be seen in the inset of Fig. 6 [46]. This limit corresponds to the maximum amount of the catalyst in which all the surface exposed is fully illuminated. For higher catalyst loadings, a screening effect occurs, which masks part of the photosensitive surface. This limit depends, among others, on the concentration of the substrate [46]. As seen in Fig. 6, at the low As(III) concentration the TiO_2 loadings tested (i.e. 50 and 250 mg/L) are close to the level off regime of the inset curve, while at the high As(III) concentration the TiO_2 loadings are located in the increasing regime of the inset curve. Therefore, at the high As(III) concentration, increasing TiO_2 loading has a more intense effect on the photocatalytic oxidation of As(III).

In the last group of relatively low significant effects, two positive effects of treatment time and solution pH and a negative interaction effect of [As(III)] × [HA] can be found. Increasing treatment time increases As(III) oxidation, which is expected although not at this relatively low score. The positive effect of solution pH indicates that As(III) oxidation in the ternary As(III)/HA/TiO_2 system is favored at near neutral pH. This result is in agreement with previous studies published in the literature for the binary As(III)/TiO_2 system reporting that As(III) oxidation increases when increasing solution pH [15,16,23] and in contrast with other studies reporting that pH had practically no influence on the photocatalytic oxidation of As(III)

[12,14,17]. However, it should be noted that the influence of solution pH in the ternary system may be complicated by the presence of HA and the influence of pH on the photocatalytic oxidation of HA (vide infra). The negative interaction effect of [As(III)] × [HA] indicates that increasing HA concentration at the low level of As(III) concentration has a lower negative effect compared to the effect at high As(III) concentration level. This negative interaction effect implies an antagonistic effect with respect to the active catalyst sites especially at high concentrations of HA and As(III).

In the case of HA photocatalytic oxidation, as can be seen in Fig. 5, there are ten important factors, which can be grouped as follows: the first group comprises two very large positive effects of HA and TiO_2 concentration and a very large negative effect of solution pH, followed by a large negative interaction effect of [HA] × pH. It should be noted that the statistical treatment of the experimental data regarding HA oxidation was performed using three wavelengths to measure HA concentration (see Section 2.3); it was found that the results obtained in terms of the statistically important parameters were the same regardless the wavelength used to measure HA concentration.

The positive effects of HA and TiO_2 concentration indicate that the greater the amount of HA and TiO_2, the greater the amount of HA oxidized. The negative effect of solution pH indicates that photocatalytic HA oxidation in the ternary As(III)/HA/TiO_2 system is favored at acidic pH. This may be attributed to the increased adsorption of HA onto the TiO_2 surface at acidic pH as this was observed in the preliminary adsorption studies (Table 1). This result is in agreement with previous studies reporting that HA photocatalytic oxidation in the binary HA/TiO_2 system is favored at acidic pH [47] and in contrast with other studies reporting that HA oxidation is favored at near neutral pH [48]. However, these results are not directly comparable to ours, because the behavior of the ternary system is different from the behavior of the binary system. The negative interaction effect of [HA] × pH indicates that increasing solution pH from acidic to near neutral has a higher negative impact on HA photocatalytic oxidation at the high level of HA concentration.

The second group of effects comprises one positive and one negative moderate interaction effects, namely [HA] × [TiO_2] and [HA] × [TiO_2] × pH respectively. The positive two-factor interaction effect of [HA] × [TiO_2] indicates that increasing catalyst loading has a higher impact on HA oxidized at the high level of HA concentration. For the three-factor negative interaction effect of [HA] × [TiO_2] × pH, it is hard to give a pictorial presentation and, more importantly, a physical meaning. The last group of relatively low significant effects comprises three positive effects, namely the three-factor interaction effect of [As(III)] × [HA] × [TiO_2], the two-factor interaction effect of [As(III)] × [TiO_2] and treatment time, and a negative two-factor interaction effect of [TiO_2] × pH. The positive effect of treatment time was expected although not at this relatively low score. The positive two-factor interaction effect of [As(III)] × [TiO_2] indicates that increasing catalyst loading has a higher impact on HA oxidized at the high level of As(III) concentration, while the negative interaction effect of [TiO_2] × pH shows that decreasing solution pH has a higher positive effect on HA oxidation at the high level of TiO_2 concentration. Moreover, it is worthwhile to point out that As(III) concentration at the values chosen in the present study (i.e. 3 and 20 mg/L) has a negligible effect on HA oxidation as can be seen from its very low effect which lies far below the margin of error. However, As(III) concentration can be found in various two- and three-factor interaction effects, as it was mentioned earlier.

3.7. Mathematical model

One of the main objectives of the experimental design technique is to obtain a mathematical model that directly relates the various response factors with the statistically significant variables and their interactions. Therefore, a first order polynomial mathematical model describing the two experimental response factors was constructed as follows:

$$Y_1 = 5.187 + \frac{6.206}{2}X_1 - \frac{3.885}{2}X_2 + \frac{4.707}{2}X_3 + \frac{2.477}{2}X_4 + \frac{2.847}{2}X_5 - \frac{2.822}{2}X_1X_2 + \frac{3.643}{2}X_1X_3 \quad (2)$$

$$Y_2 = 11.009 + \frac{9.024}{2}X_2 + \frac{8.491}{2}X_3 - \frac{8.168}{2}X_4 + \frac{1.848}{2}X_5 + \frac{1.871}{2}X_1X_3 + \frac{3.718}{2}X_2X_3 - \frac{6.183}{2}X_2X_4 - \frac{1.491}{2}X_3X_4 + \frac{2.161}{2}X_1X_2X_3 - \frac{3.433}{2}X_2X_3X_4 \quad (3)$$

where Y_1 is the concentration of As(III) oxidized in mg/L, Y_2 is the concentration of HA oxidized in mg/L and X_i are the transformed forms of the independent variables according to

$$X_i = \frac{Z_i - ((Z_{high} + Z_{low})/2)}{(Z_{high} - Z_{low})/2} \quad (4)$$

and Z_i are the original (untransformed) values of the variables.

Eq. (4) transforms the original values of the variables to $X_i = -1$ and $X_i = +1$ for the low and high values respectively. The coefficients that appear in Eqs. (2) and (3) are half the calculated effects, because a change of $X = -1$ to $X = 1$ is a change of two units along the X-axis.

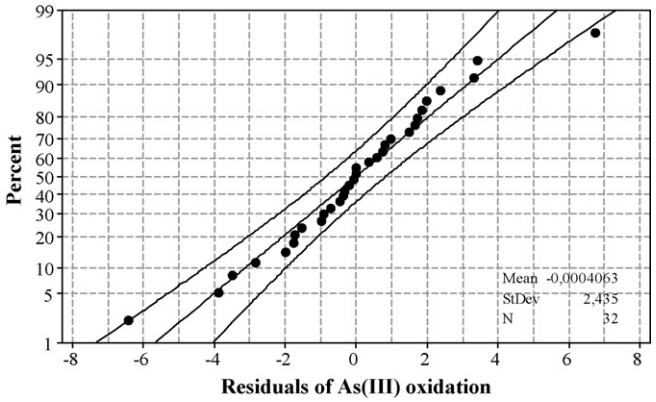

Fig. 7. Normal probability plot of the residuals at 95% confidence interval for the response factor Y_1.

3.8. Model validation

The validation of the mathematical model was based on the calculation of the residuals, which are the observed minus the predicted values according to the model, for the two response factors. The values of the calculated residuals for the two response factors were plotted in a normal probability plot and the results are shown in Figs. 7 and 8. For both responses, almost all data points lie close to a straight line and within the 95% confidence intervals lines with mean values near zero. These results indicate that the calculated residuals follow a normal distribution with mean values near zero. According to the above observations, it can be concluded that there is a good agreement between the experimental values and the simple first order polynomial mathematical model developed and the observed differences (i.e. the residuals) may be readily explained as random noise.

The empirical modeling approach presented above has two important advantages: (i) it adequately describes, in a statistical

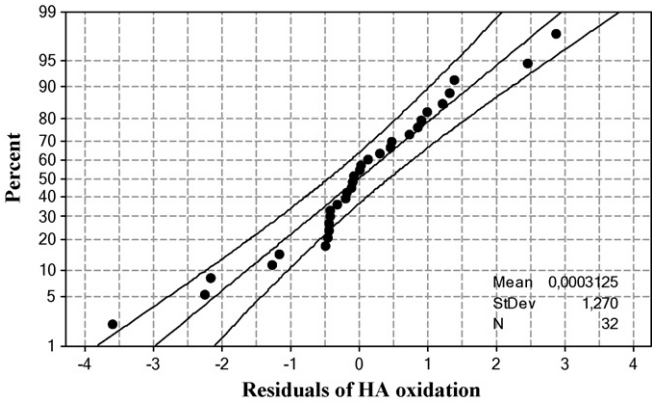

Fig. 8. Normal probability plot of the residuals at 95% confidence interval for the response factor Y_2.

sense, the system response within the values set by the operating variables, and (ii) it identifies the most important variables and interactions of variables which affect the system performance. Because the model ignores the chemistry involved, it cannot be safely used outside the operating area studied. However, the methodology presented in this work can be extended to cover other operating conditions which may exist in the natural environment.

4. Conclusions

This work investigates various parameters affecting the simultaneous photocatalytic oxidation of As(III) and HA in aqueous TiO_2 suspensions. The results are of great environmental significance in arsenic removal technologies because arsenic and HA usually coexist in groundwater and HA lowers arsenic removal efficiency. A statistical approach based on a two-level factorial design methodology is employed to elucidate the statistically important factors affecting the process as well as their interactions. The conclusions can be summarized as follows:

(1) TiO_2 photocatalysis is capable of oxidizing As(III) and HA in binary (As(III)/TiO_2 and HA/TiO_2) and ternary (As(III)/HA/TiO_2) aqueous solutions. At the experimental conditions employed in the present study, As(III) is oxidized faster than HA in the respective binary systems and the extent of photocatalytic oxidation of each individual component increases decreasing its initial concentration and/or increasing catalyst loading. For the ternary system, the photocatalytic conversion of both As(III) and HA is reduced compared to the corresponding binary systems.
(2) As(III) oxidation in the ternary system is favored at high TiO_2 loadings, low initial HA concentration, near neutral pH and longer treatment times. The process can be described by a simple, first order polynomial model yielding a very good agreement between experimental and predicted values.
(3) HA oxidation in the ternary system is favored at high TiO_2 loadings, acidic pH and longer treatment times, while the mathematical model developed for the photocatalytic HA oxidation is more complicated because a relatively high number of two- and three-factor interactions appear to be significant. However, again good agreement between experimental and predicted values is achieved.

The combination of the proposed simultaneous photocatalytic As(III) and HA oxidation with a subsequent separation stage, such as adsorption onto activated alumina and/or ZVI, could become a successful remediation technology for arsenic contamination. In this light, the mathematical model developed for the simultaneous As(III) and HA oxidation could serve as a basis to define optimal operating conditions for the integrated process.

References

[1] S. Ahuja, Arsenic Contamination of Groundwater: Mechanism, Analysis, and Remediation, John Wiley & Sons, Inc., Hoboken, New Jersey, 2008.
[2] D.K. Nordstrom, Worldwide occurrences of arsenic in ground water, Science 296 (2002) 2143–2145.
[3] IARC Monographs on the Evaluation of Carcinogenic Risks to Humans, Volume 84: Some Drinking-water Disinfectants and Contaminants, including Arsenic, WHO, IARC, Lyon, France, 2004. URL: http://monographs.iarc.fr/ENG/Monographs/vol84/volume84.pdf.
[4] J.S. Wang, C.M. Wai, Arsenic in drinking water—a global environmental problem, J. Chem. Educ. 81 (2004) 207–213.
[5] P.L. Smedley, D.G. Kinniburgh, A review of the source, behaviour and distribution of arsenic in natural waters, Appl. Geochem. 17 (2002) 517–568.
[6] P. Mondal, C.B. Majumder, B. Mohanty, Laboratory based approaches for arsenic remediation from contaminated water: recent developments, J. Hazard. Mater. 137 (2006) 464–479.
[7] N.P. Nikolaidis, G.M. Dobbs, J.A. Lackovic, Arsenic removal by zero-valent iron: field, laboratory and modeling studies, Water Res. 37 (2003) 1417–1425.
[8] K. Tyrovola, N.P. Nikolaidis, N. Veranis, N. Kallithrakas-Kontos, P.E. Koulouridakis, Arsenic removal from geothermal waters with zero-valent iron—effect of temperature, phosphate and nitrate, Water Res. 40 (2006) 2375–2386.
[9] P.K. Dutta, A.K. Ray, V.K. Sharma, F.J. Millero, Adsorption of arsenate and arsenite on titanium dioxide suspensions, J. Colloid Interface Sci. 278 (2004) 270–275.
[10] M. Pena, X. Meng, G.P. Korfiatis, C. Jing, Adsorption mechanism of arsenic on nanocrystalline titanium dioxide, Environ. Sci. Technol. 40 (2006) 1257–1262.
[11] M. Bissen, F.H. Frimmel, Arsenic—a review. Part II. Oxidation of arsenic and its removal in water treatment, Acta Hydrochim. Hydrobiol. 31 (2003) 97–107.
[12] V.K. Sharma, P.K. Dutta, A.K. Ray, Review of kinetics of chemical and photocatalytical oxidation of Asrenic(III) as influenced by pH, J. Environ. Sci. Health A 42 (2007) 997–1004.
[13] H. Yang, W.Y. Lin, K. Rajeshwar, Homogeneous and heterogeneous photocatalytic reactions involving As(III) and As(V) species in aqueous media, J. Photochem. Photobiol. A 123 (1999) 137–143.
[14] M. Bissen, M.M. Vieillard-Baron, A.J. Schindelin, F.H. Frimmel, TiO_2-catalyzed photooxidation of arsenite to arsenate in aqueous samples, Chemosphere 44 (2001) 751–757.
[15] H. Lee, W. Choi, Photocatalytic oxidation of arsenite in TiO_2 suspension: kinetics and mechanisms, Environ. Sci. Technol. 36 (2002) 3872–3878.
[16] J. Ryu, W. Choi, Effects of TiO_2 surface modifications on photocatalytic oxidation of arsenite: the role of superoxides, Environ. Sci. Technol. 38 (2004) 2928–2933.
[17] P.K. Dutta, S.O. Pehkonen, V.K. Sharma, A.K. Ray, Photocatalytic oxidation of arsenic(III): evidence of hydroxyl radicals, Environ. Sci. Technol. 39 (2005) 1827–1834.
[18] M.A. Ferguson, M.R. Hoffmann, J.G. Hering, TiO_2-photocatalyzed As(III) oxidation in aqueous suspensions: reaction kinetics and effect of adsorption, Environ. Sci. Technol. 39 (2005) 1880–1886.
[19] S.-H. Yoon, J.H. Lee, Oxidation mechanism of As(III) in the UV/TiO_2 system: evidence for a direct hole mechanism, Environ. Sci. Technol. 39 (2005) 9695–9701.
[20] T. Xu, P.V. Kamat, K.E. O'Shea, Mechanistic evaluation of arsenite oxidation in TiO_2 assisted photocatalysis, J. Phys. Chem. A 109 (2005) 9070–9075.
[21] M.A. Ferguson, J.G. Hering, TiO_2-photocatalyzed As(III) oxidation in a fixed-bed, flow-through reactor, Environ. Sci. Technol. 40 (2005) 4261–4267.
[22] J. Ryu, W. Choi, Photocatalytic oxidation of arsenite on TiO_2: understanding the controversial oxidation mechanism involving superoxides and the effect of alternative electron acceptors, Environ. Sci. Technol. 40 (2006) 7034–7039.
[23] S.-H. Yoon, J.H. Lee, Combined use of photochemical reaction and activated alumina for the oxidation and removal of arsenic(III), J. Ind. Eng. Chem. 13 (2007) 97–104.
[24] M.R. Hoffmann, S.T. Martin, W. Choi, D.W. Bahnemann, Environmental applications of semiconductor photocatalysis, Chem. Rev. 95 (1995) 69–96.
[25] A.B.M. Giasuddin, S.R. Kanel, H. Choi, Adsorption of humic acid onto nanoscale zerovalent iron and its effect on arsenic removal, Environ. Sci. Technol. 41 (2007) 2022–2027.
[26] N.P. Nikolaidis, Technical Report on Arsenic Remediation Applications in Hungary (in Greek).
[27] C.S. Uyguner, S.A. Suphandag, A. Kerc, M. Bekbolet, Evaluation of adsorption and coagulation characteristics of humic acids preceded by alternative advanced oxidation techniques, Desalination 210 (2007) 183–193.
[28] A.H. Fostier, M.S.S. Pereira, S. Rath, J.R. Guimarães, Arsenic removal from water employing heterogeneous photocatalysis with TiO_2 immobilized in PET bottles, Chemosphere 72 (2008) 319–324.
[29] J. Buschmann, S. Canonica, U. Lindauer, S.J. Hug, L. Sigg, Photoirradiation of dissolved humic acid induces arsenic(III) oxidation, Environ. Sci. Technol. 39 (2005) 9541–9546.
[30] J. Buschmann, A. Kappeler, U. Lindauer, D. Kistler, M. Berg, L. Sigg, Arsenite and arsenate binding to dissolved humic acids: influence of pH, type of humic acid, and aluminum, Environ. Sci. Technol. 40 (2006) 6015–6020.
[31] R.L. Malcolm, P. MacCarthy, Limitations in the use of commercial humic acids in water and soil research, Environ. Sci. Technol. 20 (1986) 904–911.

[32] P.A. Neale, B.I. Escher, A.I. Schäfer, pH Dependence of steroid hormone–organic matter interactions at environmental concentrations, Sci. Total Environ. 407 (2009) 1164–1173.
[33] M. Grandbois, D.E. Latch, K. Mcneill, Microheterogeneous concentrations of singlet oxygen in natural organic matter isolate solutions, Environ. Sci. Technol. 42 (2008) 9184–9190.
[34] P.A. Neale, B.I. Escher, Schäfer, Quantification of solute-solute interactions using negligible-depletion solid-phase microextraction: measuring the affinity of estradiol to bulk organic matter, Environ. Sci. Technol. 42 (2008) 2886–2892.
[35] B. Schreiber, V. Schmalz, T. Brinkmann, E. Worch, The effect of water temperature on the adsorption equilibrium of dissolved organic matter and atrazine on granular activated carbon, Environ. Sci. Technol. 41 (2007) 6448–6453.
[36] D.L. Sparks, Environmental Soil Chemistry, Academic Press, San Diego, CA, 1995.
[37] T. Tan, D. Beydoun, R. Amal, Effects of organic hole scavenger on the photocatalytic reduction of selenium anions, J. Photochem. Photobiol. A 159 (2003) 273–280.
[38] C. Fotiadis, N.P. Xekoukoulotakis, D. Mantzavinos, Photocatalytic treatment of wastewater from cottonseed processing: effect of operating conditions, aerobic biodegradability and ecotoxicity, Catal. Today 124 (2007) 247–253.
[39] J.F. Edzwald, W.C. Becker, K.L. Wattier, Surrogate parameters for monitoring organic-matter and THM precursors, J. Am. Water Works Assoc. 77 (4) (1985) 122–132.
[40] X. Meng, G.P. Korfiatis, C. Christodoulatos, S. Bang, Treatment of Bangladesh well water using a household co-precipitation and filtration system, Water Res. 35 (2001) 2508–2810.
[41] R.K. Dhar, Y. Zheng, J. Rubenstone, A. van Geen, A rapid colorimetric method for measuring arsenic concentration in groundwater, Anal. Chim. Acta 526 (2004) 203–209.
[42] G.E.P. Box, J.S. Hunter, W.G. Hunter, Statistics for Experimenters: Design, Innovations, and Discovery, 2nd ed., John Wiley & Sons, Inc., Hoboken, New Jersey, 2005.
[43] D.G. Kinniburgh, C.J. Milne, M.F. Benedetti, J.P. Pinheiro, J. Filius, L.K. Koopal, W.H. Van Riemsdijk, Metal ion binding by humic acid: application of the NICA–Donnan model, Environ. Sci. Technol. 30 (1996) 1687–1698.
[44] D. Papadam, N.P. Xekoukoulotakis, I. Poulios, D. Mantzavinos, Photocatalytic transformation of acid orange 20 and Cr(VI) in aqueous TiO_2 suspensions, J. Photochem. Photobiol. A 186 (2007) 308–315.
[45] R.V. Lenth, Quick and easy analysis of unreplicated factorials, Technometrics 31 (1989) 469–473.
[46] J.M. Hermann, Heterogeneous photocatalysis: fundamentals and applications to the removal of various types of aqueous pollutants, Catal. Today 53 (1999) 115–129.
[47] H. Selcuk, J.J. Sene, M.A. Anderson, Photoelectrocatalytic humic acid degradation kinetics and effect of pH, applied potential and inorganic ions, J. Chem. Technol. Biotechnol. 78 (2003) 979–984.
[48] F.L. Palmer, B.R. Eggins, H.M. Coleman, The effect of operational parameters on the photocatalytic degradation of humic acid, J. Photochem. Photobiol. A 148 (2002) 137–143.